

Searching for Potential Mergers among 22 500 Eclipsing Binary Stars in the OGLE-III Galactic Bulge Fields*

P. Pietrukowicz¹, I. Soszynski¹, A. Udalski¹,
 M. K. Szymanski¹, L. Wyrzykowski¹, R. Poleski^{1,2},
 S. Kozlowski¹, J. Skowron¹, P. Mróz¹, M. Pawlak¹,
 and K. Ulaczyk^{1,3}

¹ Warsaw University Observatory, Al. Ujazdowskie 4, 00-478 Warszawa,
 Poland

e-mail: pietruk@astrouw.edu.pl

² Department of Astronomy, Ohio State University, 140 W. 18th Ave.,
 Columbus, OH 43210, USA

³ Department of Physics, University of Warwick, Coventry CV4 7AL, UK

ABSTRACT

Inspired by the discovery of the red nova V1309 Sco (Nova Scorpii 2008) and the fact that its progenitor was a binary system with a rapidly decreasing orbital period, we have searched for period changes in OGLE binary stars. We have selected a sample of 22 462 short-period ($P_{\text{orb}} < 4$ d) eclipsing binary stars observed toward the Galactic bulge by the OGLE-III survey in years 2001–2009. This dataset was extended with photometry from OGLE-II (1997–2000) and the first six years of OGLE-IV (2010–2015). For some stars, the data were supplemented with OGLE-I photometry (1992–1995). After close inspection of the whole sample we have found 56 systems with realistic period decrease and 52 systems with realistic period increase. We have also recognized 35 systems with cyclic period variations. The highest negative period change rate of -1.943×10^{-4} d/y has been detected in detached eclipsing binary OGLE-BLG-ECL-139622 with $P_{\text{orb}} = 2.817$ d, while all other found systems are contact binaries with orbital periods mostly shorter than 1.0 d. For 22 our systems with decreasing orbital period the absolute rate is higher than the value reported recently for eclipsing binary KIC 9832227. Interestingly, there is an excess of systems with high negative period change rate over systems with positive rate. We cannot exclude the possibility that some of the contact binaries with relatively long orbital period and high negative period change rate will merge in the future. However, our results rather point to the presence of tertiary companions in the observed systems and/or spot activity on the surface of the binary components.

Galaxy: bulge – Galaxy: disk – binaries: eclipsing

1 Introduction

Red novae belong to a very intriguing class of rarely observed luminous transients. They are associated with a dynamical phase of common envelope evolution (Soker and Tylenda 2003), albeit alternative explanations have been also proposed, such as classical nova eruption with a slowly moving, massive envelope (Shara *et al.* 2010), or explosion of the star in the dust-enshrouded phase of the evolution at the extremum of the asymptotic giant branch (Thompson *et al.* 2009), or intensive mass loss from the binary system through the outer Lagrangian point (Pejcha 2014). So far, only a handful number of this kind of transients have been noted in the Milky Way: V4332 Sgr (Hayashi *et al.* 1994), V838 Mon (Brown *et al.* 2002), V1309 Sco (Nakano *et al.* 2008), and OGLE-2002-BLG-360 (Tylenda *et al.* 2013). Thanks to precise high-cadence OGLE

*Based on observations obtained with the 1.3-m Warsaw telescope at the Las Campanas Observatory of the Carnegie Institution for Science.

photometry covering seven years before the eruption of the red nova V1309 Sco, it was realized that the progenitor was a contact eclipsing binary with the orbital period shrinking from about 1.438 d in 2002 to 1.425 d in 2007 (Tylenda *et al.* 2011). Before the eruption, the light curve shape of the object transformed from a double wave to single wave which indicated the immersion of two stellar bodies in an elongated common envelope. According to the estimation made by Kochanek *et al.* (2014), the number of Galactic events like the V1309 Sco outburst is about once per decade.

The main goal of our work is searching for candidates for future stellar mergers or systems with high negative period change rate among eclipsing binaries observed by the OGLE survey toward the Milky Way bulge. From the sample of eclipsing binaries, we also select systems with positive period change rate and systems with noticeable cyclic period variations.

2 Observations

The Optical Gravitational Lensing Experiment (OGLE) is a long-term wide-field variability sky survey launched in 1992 with the original aim of searching for microlensing events (Udalski *et al.* 1992). The survey is conducted at Las Campanas Observatory which is operated by the Carnegie Institution for Science. OGLE uses the 1.3-m Warsaw Telescope. Since 2010 the project is in its fourth phase, OGLE-IV (Udalski *et al.* 2015), collecting data with a 32-CCD mosaic camera of a field of view of 1.4 deg². Currently, OGLE monitors over 3000 deg² of the sky. Previous phases of the project were conducted in the following years: 1992–1995 (OGLE-I), 1997–2000 (OGLE-II), and 2001–2009 (OGLE-III). In 2016 the OGLE database exceeded 10¹² single photometric measurements. The survey has discovered and classified nearly one million genuine variable stars toward the Galactic bulge, Galactic disk, and Magellanic Clouds (e.g., Soszyński *et al.* 2013, 2014, 2015, 2016, Pietrukowicz *et al.* 2013, Mróz *et al.* 2015).

Eclipsing binary systems, among which we look for potential mergers, were observed by OGLE-III in the direction of the Galactic bulge. In the third phase of OGLE, an eight-CCD mosaic camera with a field of view of about 0.35 deg² was attached to the Warsaw Telescope (Udalski *et al.* 2003). Angular pixel size in OGLE-III and OGLE-IV is the same: 0''.26. During the OGLE-III phase 267 fields covering about 92 deg² toward the Milky Way bulge were observed (Szymański *et al.* 2011). In OGLE-II, a single CCD camera with a pixel size of 0''.42 was used in driftscan mode (Udalski *et al.* 1997). In that phase, 49 Galactic bulge fields of 14''.2 × 57' each covering a total area of around 11 deg² were monitored. The bulge coverage of OGLE-I, conducted on the 1.0-m Swope telescope also at Las Campanas Observatory, was even much smaller: 18 fields of 15' × 15' each covered about 1.1 deg². OGLE monitors the sky mainly in the *I*-band, while *V*-band observations are collected to secure color information of the objects and for accurate transformation to the standard Johnson-Cousins system. The number of *I*(*V*)-band measurements in the most frequently observed Galactic bulge fields is the following: 261(44) in OGLE-I, 568(16) in OGLE-II, 2540(34) in OGLE-III, and 12 889(144) in OGLE-IV (2010–2015). Reduction of the OGLE data is performed with the difference image analysis (DIA) technique (Alard and Lupton 1998, Woźniak 2000).

3 Binary Systems Selection

For the purpose of our analysis we selected 53 OGLE-III Galactic bulge fields observed in the I -band for at least 6 seasons with a minimum number of 40 epochs per season. Location of these fields in Galactic coordinates is presented in Fig. 1. Over 28 million detections in the brightness range $12.6 < I < 19.0$ mag were a subject of the initial period search with the FNPEAKS code[†] for each season separately. For further analysis we left about 14 million detections with assessed periods in all well-covered seasons. From this sample we removed detections with signals around $1/3$ d, $1/2$ d, and 1 d being very likely daily aliases. Since we concentrate on short-period systems only, we removed objects with the initially detected periods longer than 2 d or orbital periods $P_{\text{orb}} > 4$ d. After some verification tests, we decided to work further on 1% of stars with the highest variability signal. The initial periods for about 137 500 stars were corrected with the TATRY code (Schwarzenberg-Czerny 1996). Cross-matching of this sample with the list of OGLE-III Galactic bulge RR Lyr-type stars (Soszyński *et al.* 2011) led to the rejection of about 2% of stars. RR Lyr stars, particularly of RRc type showing close-to-sinusoidal light curve shapes and with periods of a few tens of day, could contaminate our sample. We made a visual inspection of I -band light curves of around 134 700 detections. This time-consuming operation allowed us to reject other contaminants from the sample, such as spotted variables, rotating variables, and δ Sct-type pulsators. Importantly, the inspection helped us to verify the orbital periods of candidates for eclipsing binaries. We corrected our list of candidate OGLE-III eclipsing variables for artifacts and duplicates detected in adjacent fields.

In the next step, we searched for OGLE-II and OGLE-IV counterparts. OGLE-IV data used cover six seasons, from 2010 to 2015. About 43% and 95% of OGLE-III bulge binaries are present in the OGLE-II and OGLE-IV images, respectively. As in the case of the OGLE-III data, we took into account only binaries with at least 40 I -band measurements per season. Several times more frequent OGLE-IV observations allowed us to verify the classification of the variables and to correct the orbital periods determined from the OGLE-III data.

The final number of detected eclipsing binaries is 22 462. For 19 885 binaries, the OGLE-III data are extended with photometry from OGLE-IV. For 8788 binaries, the data are also extended with photometry from OGLE-II. For 7825 eclipsing binaries our dataset covers 20 years of OGLE-II, OGLE-III, and OGLE-IV. In the case of the most interesting systems, this dataset was supplemented with OGLE-I photometry increasing the time coverage up to 24 years. In our final sample, there are 1657 binaries with solely OGLE-III photometry. All light curves were cleaned from outlying points by phasing and binning the data. After some tests we set the cleaning limit at a mild level of 5σ to avoid rejection of good data points in the case of systems with possibly high period change rates. For objects that are present in the OGLE collection of eclipsing binary stars toward the Galactic bulge published by Soszyński *et al.* (2016), we use their format: OGLE-BLG-ECL-NNNNNN. For objects that are absent in that collection, we left the standard format used in the OGLE database: FIELD.CHIP.ID.

[†]<http://helas.astro.uni.wroc.pl/deliverables.php?lang=en&active=fnpeaks>

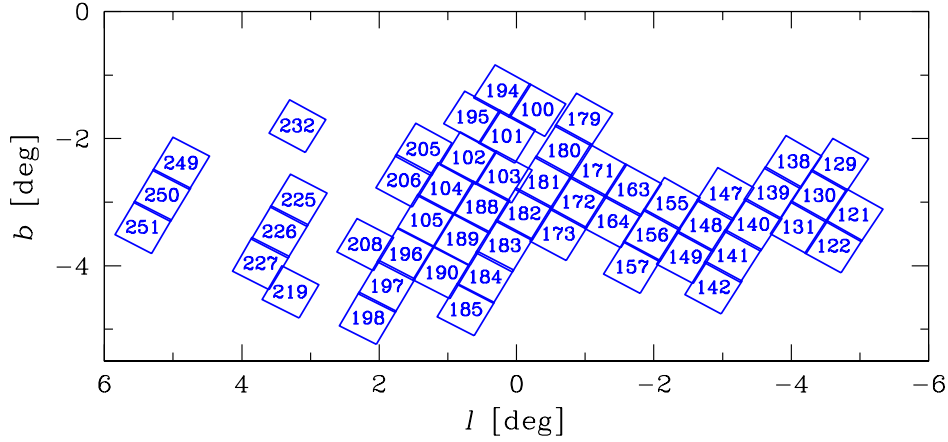


Fig. 1. Location of 53 OGLE-III Galactic bulge fields selected for eclipsing binary stars searches.

4 Period Changes

A simple method was applied to find systems with reliable period change rates and candidates for possible mergers in the sample of 22 462 eclipsing binaries. We searched for negative as well as positive linear period changes using I -band photometry from OGLE-II, OGLE-III, and OGLE-IV, depending on the coverage. OGLE-III and OGLE-IV data were divided into seasons. After some tests we decided not to divide the less rich OGLE-II data. For each OGLE-III/IV season and the whole four-year OGLE-II dataset accurate orbital periods were determined using the TTRY code (Schwarzenberg-Czerny 1996). Moments corresponding to each period of time were calculated as average from the epochs. Our approach allowed us to avoid possible problems with variations in mean brightness, amplitude, and light curve shapes (due to star spots), also problems with the presence of some remnant outlying points near eclipses and small magnitude offsets between the photometry from different OGLE phases to all of which the classical $O-C$ method is sensitive (e.g., Conroy *et al.* 2014, Gies *et al.* 2015 in the application to data from the Kepler satellite). After fitting a linear regression to all obtained “period change curves”, we made a close inspection of 2403 systems for which $|\dot{P}_{\text{orb}}| > 5\sigma_{\dot{P}_{\text{orb}}}$. In many period change curves with particularly high rate derived from the automated fit, we noticed outlying points corresponding to less frequently observed seasons. After the inspection we found only 59 systems with realistic period decrease and 53 systems with realistic period increase. We identified 35 systems with evident cyclic period variations.

In the last stage, we verified whether some of the found interesting binaries had been observed by OGLE-I in years 1992–1995. Photometry was collected for twelve of these binaries. It turned out that three candidate systems with decreasing period and one candidate system with increasing period seem to show rather non-monotonic variations. The final number of detected systems with the increasing, decreasing, and cyclic period changes is 56, 52, and 35 objects, respectively.

We recognized four of our systems in the list of 569 contact binaries with reliable period change rates determined by Kubiak *et al.* (2006) based on OGLE

data from years 1992–2005. Systems BW1.125206 = OGLE-BLG-ECL-265310 and BWC.169286 = OGLE-BLG-ECL-276943 were found, at that time, to have the decreasing period, while systems BW7.159932 = OGLE-BLG-ECL-288099 and BW4.5243 = OGLE-BLG-ECL-279991 to have the increasing period. However, observations spanning 24 years indicate non-monotonic variations of the period in these four binaries.

Period change curves together with phased *I*-band light curves for seven of our binary stars with the highest negative orbital period change rate are presented in Fig. 2. In Table 1, we list basic parameters of all 56 systems with reliable negative period changes sorted from the highest absolute rate. The given orbital periods correspond roughly to the middle of the OGLE-III phase (year 2005). System OGLE-BLG-ECL-139622 with the highest derived negative period change rate of $\dot{P}_{\text{orb}} = -1.943 \times 10^{-4}$ d/y is a detached eclipsing binary of Algol (EA) type. Unfortunately, this object was monitored only in the OGLE-III phase. New time-series data would help in verification of the observed trend. Other systems with the decreasing orbital period are contact binaries. All of them have absolute rates at least one order of magnitude lower than OGLE-BLG-ECL-139622. Interestingly, high negative period change rates are observed in contact systems with relatively long orbital periods: all four contact binaries with $P_{\text{orb}} > 1.0$ d have $|\dot{P}_{\text{orb}}| > 10^{-5}$ d/y; all seven contact binaries with $P_{\text{orb}} > 0.8$ d have $|\dot{P}_{\text{orb}}| > 6 \times 10^{-6}$ d/y.

In Fig. 3, we present seven binaries with the highest derived positive period change rate. Table 2 provides information on all 52 systems with the increasing orbital period. All such systems have the orbital period < 0.8 d and the period change rate $< 10^{-5}$ d/y or lower than the absolute value in eight systems with the most rapid negative period changes. Distributions of systems with negative and positive period change rates are compared in Fig. 4. All detected systems with the increasing orbital period are contact binaries.

Finally, in Fig. 5 and Table 3, we present systems with cyclic period variations. We assess the cycle period for each of the system. All these systems are contact binaries with $P_{\text{orb}} < 0.9$ d.

5 Summary and Conclusions

In the huge sample of 22 462 eclipsing binaries with $P_{\text{orb}} < 4$ d detected in the OGLE-III Galactic bulge fields, we found 108 systems with reliable monotonic period changes: 56 systems with negative rate and 52 systems with positive one. We also indicated 35 systems with evident cyclic period variations. All reported systems but object OGLE-BLG-ECL-139622 with the highest derived negative period change rate are contact binaries. We did not find any binary with rapid orbital period decrease as expected for a system heading toward merger within a few years. The period change rate in V1309 Sco five years before the merger event was about -8.3×10^{-4} d/y, while two years before the event it reached -3.8×10^{-3} d/y. For comparison, contact binary OGLE-BLG-ECL-299145 with the second fastest measured period decrease in the whole our sample has the rate of merely -1.7×10^{-5} d/y. Twenty-two our systems with negative period changes have the absolute rate higher than -2×10^{-6} d/y, that is the value estimated for contact system KIC 9832227 by Molnar *et al.* (2017). We cannot exclude the possibility that this particular binary system and also our contact binaries with relatively long orbital period ($P_{\text{orb}} > 1.0$ d) and relatively high negative period change rate ($|\dot{P}_{\text{orb}}| > 10^{-5}$ d/y), such as OGLE-BLG-ECL-344477,

Table 1: Parameters of the systems with derived negative period change rate

OGLE-BLG-ECL-	RA J2000.0	Dec J2000.0	I_{\max} [mag]	$V - I$ [mag]	P_{orb} [d]	P_{orb} [d/y]
139622	17 ^h 51 ^m 33 ^s .33	-29°54'38.7"	15.28	1.41	2.817436	-1.94 ± 0.28 E-4
299145	18 ^h 05 ^m 34 ^s .20	-29°40'21.5"	16.42	1.26	1.252603	-1.72 ± 0.24 E-5
344477	18 ^h 10 ^m 24 ^s .89	-28°34'26.5"	16.08	1.23	1.032195	-1.50 ± 0.18 E-5
176377	17 ^h 54 ^m 41 ^s .59	-29°29'18.1"	16.80	1.74	1.245946	-1.42 ± 0.05 E-5
339765	18 ^h 09 ^m 52 ^s .64	-27°25'53.1"	18.62	1.47	0.377840	-1.18 ± 0.08 E-5
170070	17 ^h 54 ^m 09 ^s .38	-29°42'53.7"	16.43	1.85	1.401907	-1.15 ± 0.03 E-5
175354	17 ^h 54 ^m 36 ^s .55	-33°44'51.9"	17.31	1.58	0.840163	-1.06 ± 0.16 E-5
154749	17 ^h 52 ^m 54 ^s .10	-29°08'29.7"	17.55	2.45	0.932247	-1.04 ± 0.18 E-5
220028	17 ^h 58 ^m 24 ^s .67	-29°57'42.0"	16.68	1.53	0.920792	-6.02 ± 1.10 E-6
172659	17 ^h 54 ^m 22 ^s .13	-30°01'41.9"	18.10	1.77	0.626226	-5.85 ± 0.21 E-6
195664	17 ^h 56 ^m 19 ^s .97	-30°55'40.9"	18.55	1.71	0.436900	-4.56 ± 0.19 E-6
192939	17 ^h 56 ^m 06 ^s .40	-29°29'21.4"	18.23	2.09	0.531934	-4.40 ± 0.20 E-6
243151	18 ^h 00 ^m 27 ^s .01	-29°27'41.1"	18.41	1.62	0.403628	-4.35 ± 0.50 E-6
347999	18 ^h 10 ^m 49 ^s .69	-29°25'35.8"	18.39	1.31	0.365383	-4.30 ± 0.66 E-6
212252	17 ^h 57 ^m 44 ^s .48	-31°03'40.8"	18.71	1.95	0.413250	-3.88 ± 0.17 E-6
168049	17 ^h 53 ^m 59 ^s .85	-30°07'37.4"	17.66	1.64	0.506522	-2.71 ± 0.18 E-6
320382	18 ^h 07 ^m 43 ^s .53	-25°42'42.8"	17.31	1.68	0.388373	-2.63 ± 0.40 E-6
218785	17 ^h 58 ^m 18 ^s .73	-32°12'24.8"	18.04	1.82	0.353455	-2.53 ± 0.36 E-6
119460	17 ^h 49 ^m 11 ^s .03	-35°01'02.8"	17.12	1.41	0.394387	-2.49 ± 0.36 E-6
351804	18 ^h 11 ^m 16 ^s .73	-25°42'55.4"	16.71	1.46	0.385420	-2.12 ± 0.26 E-6
130708	17 ^h 50 ^m 35 ^s .67	-29°19'13.6"	17.49	2.10	0.366826	-2.05 ± 0.39 E-6
149279	17 ^h 52 ^m 26 ^s .28	-32°13'12.7"	17.62	2.08	0.314728	-2.03 ± 0.32 E-6
183004	17 ^h 55 ^m 16 ^s .99	-31°03'52.4"	15.73	1.37	0.467429	-2.03 ± 0.10 E-6
190636	17 ^h 55 ^m 55 ^s .09	-31°00'26.6"	17.63	1.85	0.305221	-1.96 ± 0.16 E-6
287671	18 ^h 04 ^m 31 ^s .54	-28°38'06.5"	17.08	1.19	0.532926	-1.94 ± 0.07 E-6
201682	17 ^h 56 ^m 50 ^s .80	-29°44'49.5"	17.32	1.90	0.497314	-1.89 ± 0.29 E-6
213011	17 ^h 57 ^m 48 ^s .50	-29°21'59.0"	17.65	1.94	0.573979	-1.78 ± 0.11 E-6
159116	17 ^h 53 ^m 16 ^s .11	-29°48'59.7"	15.83	1.26	0.587393	-1.72 ± 0.06 E-6
229500	17 ^h 59 ^m 13 ^s .78	-30°49'06.9"	16.01	1.56	0.398365	-1.71 ± 0.19 E-6
163655	17 ^h 53 ^m 38 ^s .86	-32°55'59.1"	17.00	1.70	0.492482	-1.62 ± 0.09 E-6
192437	17 ^h 56 ^m 03 ^s .96	-29°59'12.6"	16.71	1.67	0.402313	-1.60 ± 0.07 E-6
233821	17 ^h 59 ^m 37 ^s .95	-28°50'22.4"	15.29	1.23	0.359920	-1.59 ± 0.04 E-6
238356	18 ^h 00 ^m 01 ^s .26	-29°09'07.4"	17.23	1.52	0.292658	-1.47 ± 0.05 E-6
176119	17 ^h 54 ^m 40 ^s .35	-29°56'26.1"	16.37	1.68	0.594569	-1.44 ± 0.06 E-6
181311	17 ^h 55 ^m 08 ^s .47	-29°33'46.8"	16.51	1.37	0.422617	-1.43 ± 0.05 E-6
217990	17 ^h 58 ^m 14 ^s .55	-31°30'12.7"	18.39	1.83	0.412545	-1.14 ± 0.17 E-6
182438	17 ^h 55 ^m 14 ^s .05	-30°10'56.0"	17.54	1.75	0.549392	-1.11 ± 0.09 E-6
280295	18 ^h 03 ^m 51 ^s .13	-27°54'12.3"	16.19	1.35	0.484237	-1.10 ± 0.10 E-6
181083	17 ^h 55 ^m 07 ^s .21	-29°58'17.8"	16.20	1.45	0.349391	-1.02 ± 0.04 E-6
114280	17 ^h 48 ^m 28 ^s .67	-35°05'09.9"	16.30	1.28	0.453031	-9.99 ± 1.64 E-7
106230	17 ^h 47 ^m 21 ^s .97	-34°40'49.3"	16.06	1.32	0.489019	-8.88 ± 0.45 E-7
184767	17 ^h 55 ^m 25 ^s .22	-29°56'15.9"	17.38	2.42	0.473305	-8.57 ± 1.18 E-7
225278	17 ^h 58 ^m 52 ^s .64	-28°42'13.3"	16.96	1.36	0.417923	-7.21 ± 0.55 E-7
241306	18 ^h 00 ^m 17 ^s .74	-29°16'25.1"	14.38	1.09	0.371268	-7.11 ± 0.22 E-7
246693	18 ^h 00 ^m 46 ^s .32	-28°52'27.3"	15.69	0.84	0.363524	-7.01 ± 0.32 E-7
122558	17 ^h 49 ^m 35 ^s .14	-30°48'09.5"	16.79	1.92	0.410946	-6.79 ± 1.20 E-7
162594	17 ^h 53 ^m 33 ^s .56	-30°03'08.9"	16.79	1.70	0.356191	-6.24 ± 0.26 E-7
207879	17 ^h 57 ^m 22 ^s .78	-28°56'59.1"	15.10	1.48	0.393082	-5.51 ± 0.33 E-7
215121	17 ^h 58 ^m 00 ^s .28	-29°57'49.2"	17.46	1.59	0.307842	-5.51 ± 1.13 E-7
250731	18 ^h 01 ^m 07 ^s .03	-30°42'13.7"	16.63	1.69	0.260272	-4.91 ± 0.57 E-7
294795	18 ^h 05 ^m 10 ^s .60	-29°21'03.9"	13.04	1.02	0.293658	-4.84 ± 0.41 E-7
198303	17 ^h 56 ^m 33 ^s .75	-30°14'33.8"	14.81	1.20	0.438734	-3.81 ± 0.72 E-7
168012	17 ^h 53 ^m 50 ^s .73	-30°04'48.6"	16.40	1.58	0.371039	-3.81 ± 0.68 E-7
279326	18 ^h 03 ^m 46 ^s .01	-29°47'40.6"	15.77	1.52	0.227733	-3.29 ± 0.24 E-7
187430	17 ^h 55 ^m 38 ^s .54	-29°17'24.1"	17.47	2.01	0.275312	-3.18 ± 0.54 E-7
217596	17 ^h 58 ^m 12 ^s .70	-28°48'16.6"	15.91	1.35	0.354705	-3.06 ± 0.13 E-7

Table 2: Parameters of the systems with derived positive period change rate

OGLE-BLG-ECL-	RA	Dec	I_{\max}	$V - I$	P_{orb}	\dot{P}_{orb}
	J2000.0	J2000.0	[mag]	[mag]	[d]	[d/y]
145302	17 ^h 52 ^m 04 ^s .81	-30°35'24"0	18.74	2.89	0.518252	7.91 ± 1.32 E-6
154461	17 ^h 52 ^m 52 ^s .57	-30°57'27"1	18.80	1.84	0.457895	7.48 ± 0.82 E-6
291221	18 ^h 04 ^m 50 ^s .83	-29°33'26"4	18.16	1.92	0.389955	4.95 ± 0.85 E-6
311367	18 ^h 06 ^m 47 ^s .01	-30°47'49"2	17.94	1.44	0.420201	4.44 ± 0.80 E-6
325941	18 ^h 08 ^m 19 ^s .42	-26°00'05"2	16.84	1.62	0.326240	4.39 ± 0.21 E-6
BLG157.1.71541	17 ^h 58 ^m 30 ^s .84	-32°39'53"8	18.68	1.91	0.268803	4.02 ± 0.59 E-6
317088	18 ^h 07 ^m 22 ^s .46	-29°18'39"2	17.68	1.33	0.487443	3.47 ± 0.69 E-6
183497	17 ^h 55 ^m 19 ^s .37	-32°55'41"0	17.77	1.18	0.523197	3.36 ± 0.79 E-6
126797	17 ^h 50 ^m 07 ^s .17	-30°09'38"1	17.75	2.56	0.367062	3.36 ± 0.57 E-6
306303	18 ^h 06 ^m 16 ^s .05	-29°00'46"8	17.88	1.15	0.415518	3.31 ± 0.59 E-6
243435	18 ^h 00 ^m 28 ^s .54	-30°27'58"7	18.31	1.56	0.419818	3.25 ± 0.58 E-6
201168	17 ^h 56 ^m 48 ^s .09	-29°30'10"7	18.16	1.92	0.465644	2.90 ± 0.56 E-6
200942	17 ^h 56 ^m 46 ^s .93	-30°00'57"6	18.30	2.08	0.358376	2.86 ± 0.52 E-6
122590	17 ^h 49 ^m 35 ^s .42	-30°32'44"1	16.33	1.48	0.306970	2.36 ± 0.10 E-6
169859	17 ^h 54 ^m 08 ^s .29	-29°44'38"1	18.13	1.50	0.393950	2.34 ± 0.13 E-6
245597	18 ^h 00 ^m 40 ^s .49	-28°39'52"1	17.99	1.50	0.402376	2.29 ± 0.11 E-6
197927	17 ^h 56 ^m 32 ^s .09	-29°15'43"0	17.22	1.76	0.545565	2.26 ± 0.27 E-6
203756	17 ^h 57 ^m 00 ^s .79	-29°39'38"4	17.95	1.71	0.418336	2.14 ± 0.41 E-6
192324	17 ^h 56 ^m 03 ^s .39	-29°25'10"6	17.81	2.02	0.436902	2.05 ± 0.24 E-6
282055	18 ^h 04 ^m 00 ^s .73	-28°39'33"7	17.61	1.39	0.482814	2.04 ± 0.14 E-6
BLG206.4.258074	18 ^h 00 ^m 56 ^s .13	-28°35'56"0	18.07	1.66	0.405867	2.00 ± 0.22 E-6
216089	17 ^h 58 ^m 05 ^s .00	-28°38'34"9	15.77	1.48	0.490068	1.92 ± 0.12 E-6
196868	17 ^h 56 ^m 26 ^s .44	-29°18'34"7	16.12	1.70	0.400507	1.86 ± 0.09 E-6
233754	17 ^h 59 ^m 37 ^s .55	-29°12'27"8	16.86	1.35	0.570240	1.84 ± 0.09 E-6
157410	17 ^h 53 ^m 07 ^s .74	-30°27'52"4	15.39	1.35	0.363414	1.69 ± 0.08 E-6
124567	17 ^h 49 ^m 50 ^s .90	-29°38'17"9	16.20	1.78	0.400343	1.61 ± 0.03 E-6
233878	17 ^h 59 ^m 38 ^s .27	-28°45'47"8	13.80	0.92	0.741434	1.60 ± 0.04 E-6
194517	17 ^h 56 ^m 14 ^s .16	-29°43'37"7	17.20	1.57	0.421592	1.58 ± 0.20 E-6
340259	18 ^h 09 ^m 55 ^s .74	-29°33'39"6	14.77	0.79	0.453261	1.38 ± 0.19 E-6
199259	17 ^h 56 ^m 38 ^s .43	-29°48'45"8	13.74	0.97	0.389284	1.37 ± 0.09 E-6
270325	18 ^h 02 ^m 56 ^s .52	-30°17'39"6	16.59	1.38	0.381891	1.32 ± 0.11 E-6
230641	17 ^h 59 ^m 20 ^s .86	-28°46'18"7	15.56	1.24	0.382904	1.29 ± 0.03 E-6
195044	17 ^h 56 ^m 16 ^s .92	-30°44'39"6	16.39	1.47	0.409737	1.16 ± 0.03 E-6
135055	17 ^h 51 ^m 04 ^s .99	-29°40'10"7	15.75	1.69	0.522241	1.10 ± 0.13 E-6
153698	17 ^h 52 ^m 48 ^s .61	-29°06'42"9	16.72	1.69	0.386626	1.08 ± 0.14 E-6
234160	17 ^h 59 ^m 39 ^s .66	-29°05'13"9	16.94	1.35	0.528657	1.06 ± 0.06 E-6
200313	17 ^h 56 ^m 43 ^s .77	-30°49'34"2	17.24	1.54	0.479131	1.03 ± 0.05 E-6
174839	17 ^h 54 ^m 34 ^s .06	-29°24'38"3	16.42	1.46	0.461225	9.62 ± 0.24 E-7
219977	17 ^h 58 ^m 24 ^s .47	-28°41'05"4	15.62	1.65	0.486807	8.94 ± 0.31 E-7
127233	17 ^h 50 ^m 10 ^s .38	-35°02'26"6	16.73	1.44	0.350237	8.74 ± 1.59 E-7
205743	17 ^h 57 ^m 12 ^s .10	-29°56'21"1	15.75	1.40	0.300489	8.24 ± 0.97 E-7
212539	17 ^h 57 ^m 45 ^s .97	-29°12'04"9	17.61	1.79	0.286102	8.15 ± 1.49 E-7
317072	18 ^h 07 ^m 22 ^s .35	-29°42'13"1	15.53	1.25	0.353712	7.28 ± 0.82 E-7
162146	17 ^h 53 ^m 31 ^s .37	-29°53'13"0	17.13	1.87	0.410687	5.97 ± 0.62 E-7
125481	17 ^h 49 ^m 57 ^s .46	-29°16'03"0	15.08	1.60	0.358558	5.88 ± 0.27 E-7
207420	17 ^h 57 ^m 20 ^s .44	-30°36'58"6	14.27	1.02	0.254388	5.63 ± 0.11 E-7
158555	17 ^h 53 ^m 13 ^s .46	-31°13'56"5	17.60	1.96	0.231003	5.44 ± 0.48 E-7
284531	18 ^h 04 ^m 14 ^s .75	-29°52'19"8	13.56	0.93	0.435555	5.17 ± 0.21 E-7
159557	17 ^h 53 ^m 18 ^s .25	-29°53'13"3	14.37	0.98	0.522287	5.01 ± 0.27 E-7
202706	17 ^h 56 ^m 55 ^s .80	-28°39'16"6	15.88	1.68	0.449735	4.08 ± 0.71 E-7
182350	17 ^h 55 ^m 13 ^s .65	-29°26'44"8	15.55	1.29	0.282379	3.46 ± 0.16 E-7
181955	17 ^h 55 ^m 11 ^s .74	-30°02'12"1	16.14	1.41	0.414302	2.62 ± 0.14 E-7

OGLE-BLG-ECL-176377, and OGLE-BLG-ECL-170070, will merge in near future (in tens or hundreds of years). However, the fact that eclipsing binary OGLE-BLG-ECL-139622 with the highest derived period change rate in our

Table 3: Parameters of candidate systems with cyclic period variations

OGLE-BLG-ECL-	RA J2000.0	Dec J2000.0	I_{\max} [mag]	$V - I$ [mag]	P_{orb} [d]	P_{cyc} [y]
124213	17 ^h 49 ^m 48 ^s 43	-33°44'49"2	18.34	1.96	0.83464370	6
124728	17 ^h 49 ^m 51 ^s 95	-29°41'48"8	17.35	2.10	0.35675024	6.5
125525	17 ^h 49 ^m 57 ^s 66	-34°39'54"5	14.76	1.20	0.41200122	15
127744	17 ^h 50 ^m 14 ^s 07	-30°06'22"3	14.98	1.77	0.89206984	6.5
129787	17 ^h 50 ^m 29 ^s 23	-29°42'24"8	16.43	2.11	0.60583946	7
144092	17 ^h 51 ^m 58 ^s 17	-29°46'41"5	15.54	1.58	0.37023316	5
148291	17 ^h 52 ^m 21 ^s 01	-29°46'59"3	16.94	1.59	0.33885024	21
153387	17 ^h 52 ^m 47 ^s 02	-33°14'16"0	18.09	1.78	0.41679258	14
154199	17 ^h 52 ^m 51 ^s 23	-29°46'23"6	16.29	1.50	0.35765448	9
157195	17 ^h 53 ^m 06 ^s 58	-30°06'54"9	16.25	1.59	0.30197516	3.0
163206	17 ^h 53 ^m 36 ^s 89	-32°43'33"6	17.65	—	0.32505982	16
163661	17 ^h 53 ^m 38 ^s 87	-29°39'03"8	18.56	1.81	0.30801484	6.5
163907	17 ^h 53 ^m 40 ^s 05	-30°07'16"9	15.25	1.37	0.28606972	7
168647	17 ^h 54 ^m 02 ^s 50	-33°00'18"2	16.10	1.65	0.31771956	10
171861	17 ^h 54 ^m 18 ^s 15	-29°33'30"8	17.62	2.03	0.33601454	2.0
174546	17 ^h 54 ^m 32 ^s 42	-29°34'58"1	15.66	1.31	0.45498264	20
177307	17 ^h 54 ^m 46 ^s 24	-29°44'55"2	17.08	1.64	0.29253374	9
184596	17 ^h 55 ^m 24 ^s 33	-29°33'41"8	13.57	0.98	0.52178366	1.5
192607	17 ^h 56 ^m 04 ^s 85	-30°20'50"3	18.06	2.46	0.36283864	4
194120	17 ^h 56 ^m 12 ^s 29	-30°46'02"8	15.93	1.47	0.31553406	5.5
207113	17 ^h 57 ^m 19 ^s 01	-33°53'47"1	17.23	1.13	0.44961886	2.7
208059	17 ^h 57 ^m 23 ^s 64	-30°49'15"3	16.52	1.53	0.41324802	1.5
209299	17 ^h 57 ^m 29 ^s 74	-30°53'29"3	16.76	1.72	0.29563266	10
219570	17 ^h 58 ^m 22 ^s 46	-29°45'49"1	16.48	1.39	0.31779704	5
222038	17 ^h 58 ^m 35 ^s 09	-29°53'02"3	18.38	1.77	0.34785152	4.5
224344	17 ^h 58 ^m 47 ^s 91	-26°50'46"5	15.38	1.52	0.39265194	9.5
235487	17 ^h 59 ^m 46 ^s 18	-29°16'00"4	15.90	1.35	0.46023396	6.5
240451	18 ^h 00 ^m 13 ^s 09	-29°14'25"9	16.70	1.39	0.36804430	22
246852	18 ^h 00 ^m 47 ^s 15	-28°36'58"2	17.57	1.55	0.42095148	8.5
250500	18 ^h 01 ^m 05 ^s 72	-30°13'22"7	18.27	1.71	0.47156330	7
289401	18 ^h 04 ^m 41 ^s 02	-28°46'03"7	16.91	1.22	0.48576687	2.8
290247	18 ^h 04 ^m 45 ^s 58	-29°31'37"7	16.36	1.47	0.40756464	5
292769	18 ^h 04 ^m 59 ^s 46	-30°36'47"3	16.92	1.86	0.24031322	5
313336	18 ^h 06 ^m 58 ^s 97	-27°41'34"2	18.70	1.60	0.32255660	3.5
314765	18 ^h 07 ^m 07 ^s 94	-29°39'00"9	14.63	1.02	0.30319922	6.5

sample is a detached system and all the remaining binaries with reliable period changes are short-period contact binaries, some of which show cyclic variations, strongly indicate for the presence of third bodies in the investigated systems. Results from various observations of nearby close binaries ($P_{\text{orb}} < 1.0$ d) support the idea that tertiary companions to such binaries are very common (D'Angelo *et al.* 2006, Pribulla and Rucinski 2006, Tokovinin *et al.* 2006, Rucinski *et al.* 2007).

Another possible explanation of the observed period changes could be slow movement of starspots on the surface of the binary components. Close binary systems are often chromospherically active and thus they can be strong X-ray emitters. We looked for X-ray counterparts to our 143 eclipsing binaries with the detected period changes and we found that all 32 binaries located within the Chandra Galactic Bulge Survey area ($-3^{\circ} \lesssim l \lesssim 3^{\circ}$, $1^{\circ} \lesssim |b| \lesssim 2^{\circ}$, Jonker *et al.* 2011, Wevers *et al.* 2016) have such counterparts. Four other binaries have counterparts in the XMM-Newton data (Page *et al.* 2012). Slowly drifting starspots would result in long-term brightness variations in the light curves of binaries. Some of our objects exhibit such mean brightness variations (see

examples in Fig. 6).

The negative result of our search for contact systems with rapid period decrease in the OGLE-III data is in agreement with the lack of observed Galactic red nova outbursts during the current fourth phase of OGLE. Despite our unsuccessful search for future mergers, binaries with relatively long orbital period and high negative period change rate are worth further monitoring.

Acknowledgments. We would like to thank Profs. M. Kubiak and G. Pietrzyński, former members of the OGLE team, for their contribution to the collection of the OGLE photometric data over the past years. The OGLE project has received funding from the National Science Centre, Poland, grant MAESTRO 2014/14/A/ST9/00121 to A.U. This work has been also supported by the Polish Ministry of Sciences and Higher Education grants No. IP2012 005672 under the Iuventus Plus program to P.P. and No. IdP2012 000162 under the Ideas Plus program to I.S.

REFERENCES

Alard, C., and Lupton, R.H. 1998, *Astrophys. J.*, **503**, 325.
 Brown, N.J., Waagen, E.O., Scovil, C., Nelson, P., Oksanen, A., Solonen, J., and Price, A. 2002, *IAU Circ.*, **7785**, 1.
 Conroy, K.E., Prša, A., Stassun, K.G., Orosz, J.A., Fabrycky, D.C., and Welsh, W.F. 2014, *Astron. J.*, **147**, 45.
 D'Angelo, C., van Kerkwijk, M.H., and Rucinski, S.M. 2006, *Astron. J.*, **132**, 650.
 Gies, D.R., Matson, R.A., Guo, Z., Lester, K.V., Orosz, J.A., and Peters, G.J. 2015, *Astron. J.*, **150**, 178.
 Hayashi, S.S., Yamamoto, M., and Hirosawa, K. 1994, *IAU Circ.*, **5942**, 1.
 Jonker, P.G., et al. 2011, *Astrophys. J. Suppl. Ser.*, **194**, 18.
 Kochanek, C.S., Adams, S.M., and Belczynski, K. 2014, *MNRAS*, **443**, 1319.
 Kubiak, M., Udalski, A., and Szymański, M.K. 2006, *Acta Astron.*, **56**, 253.
 Molnar, L.A. et al. 2017, *Astrophys. J.*, **840**, 1.
 Mróz, P., et al. 2015, *Acta Astron.*, **65**, 313.
 Nakano, S., Nishiyama, K., Kabashima, F., and Sakurai, Y. 2008, *Central Bureau Electronic Telegrams*, **1496**, 1.
 Page, M. J., et al. 2012, *MNRAS*, **426**, 903.
 Pejcha, O. 2014, *Astrophys. J.*, **788**, 22.
 Pietrukowicz, P., et al. 2013, *Acta Astron.*, **63**, 115.
 Pribulla, T., and Rucinski, S.M. 2006, *Astron. J.*, **131**, 2986.
 Rucinski, S.M., Pribulla, T., and van Kerkwijk, M.H. 2007, *Astron. J.*, **134**, 2353.
 Schwarzenberg-Czerny, A. 1996, *Astrophys. J.*, **460**, L107.
 Shara, M.M., Yaron, O., Prialnik, D., Kovetz, A., and Zurek, D. 2010, *Astrophys. J.*, **725**, 831.
 Soker, N., and Tylenda, R. 2003, *Astrophys. J.*, **582**, L105.
 Soszyński, I., et al. 2011, *Acta Astron.*, **61**, 1.
 Soszyński, I., et al. 2013, *Acta Astron.*, **63**, 21.
 Soszyński, I., et al. 2014, *Acta Astron.*, **64**, 177.
 Soszyński, I., et al. 2015, *Acta Astron.*, **65**, 39.
 Soszyński, I., et al. 2016, *Acta Astron.*, **66**, 405.
 Szymański, M.K., et al. 2011, *Acta Astron.*, **61**, 83.
 Thompson, T.A., Prieto, J.L., Stanek, K.Z., Kistler, M.D., Beacom, J.F., and Kochanek, C.S. 2009, *Astrophys. J.*, **705**, 1364.
 Tokovinin, A., Thomas, S., Sterzik, M., and Udry, S. 2006, *Astron. Astrophys.*, **450**, 681.
 Tylenda, R., et al. 2011, *Astron. Astrophys.*, **528A**, 114.
 Tylenda, R., et al. 2013, *Astron. Astrophys.*, **555**, A16.
 Udalski, A., Szymański, M., Kahužny, J., Kubiak, M., and Mateo, M. 1992, *Acta Astron.*, **42**, 253.
 Udalski, A., Kubiak, M., and Szymański, M.K. 1997, *Acta Astron.*, **47**, 169.
 Udalski, A. 2003, *Acta Astron.*, **53**, 291.
 Udalski, A., Szymański, M.K., and Szymański, G. 2015, *AA*, **65**, 1.
 Wevers, T., et al. 2016, *MNRAS*, **458**, 4530.

Woźniak, P.R. 2000, *Acta Astron.*, **50**, 421.

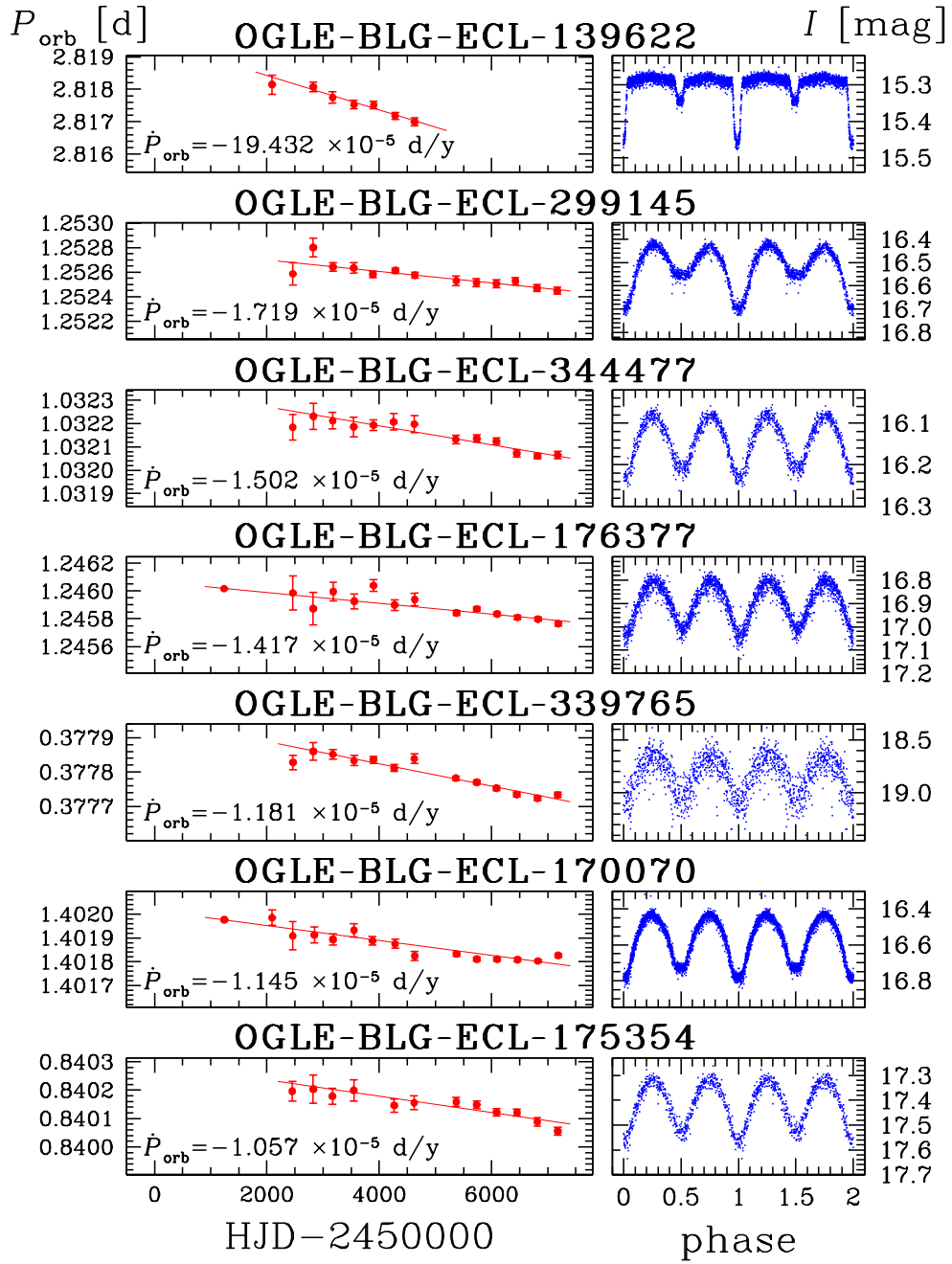


Fig. 2. Binary systems with the highest negative period change rates. Presented OGLE-III light curves are phased with constant period determined for this dataset.

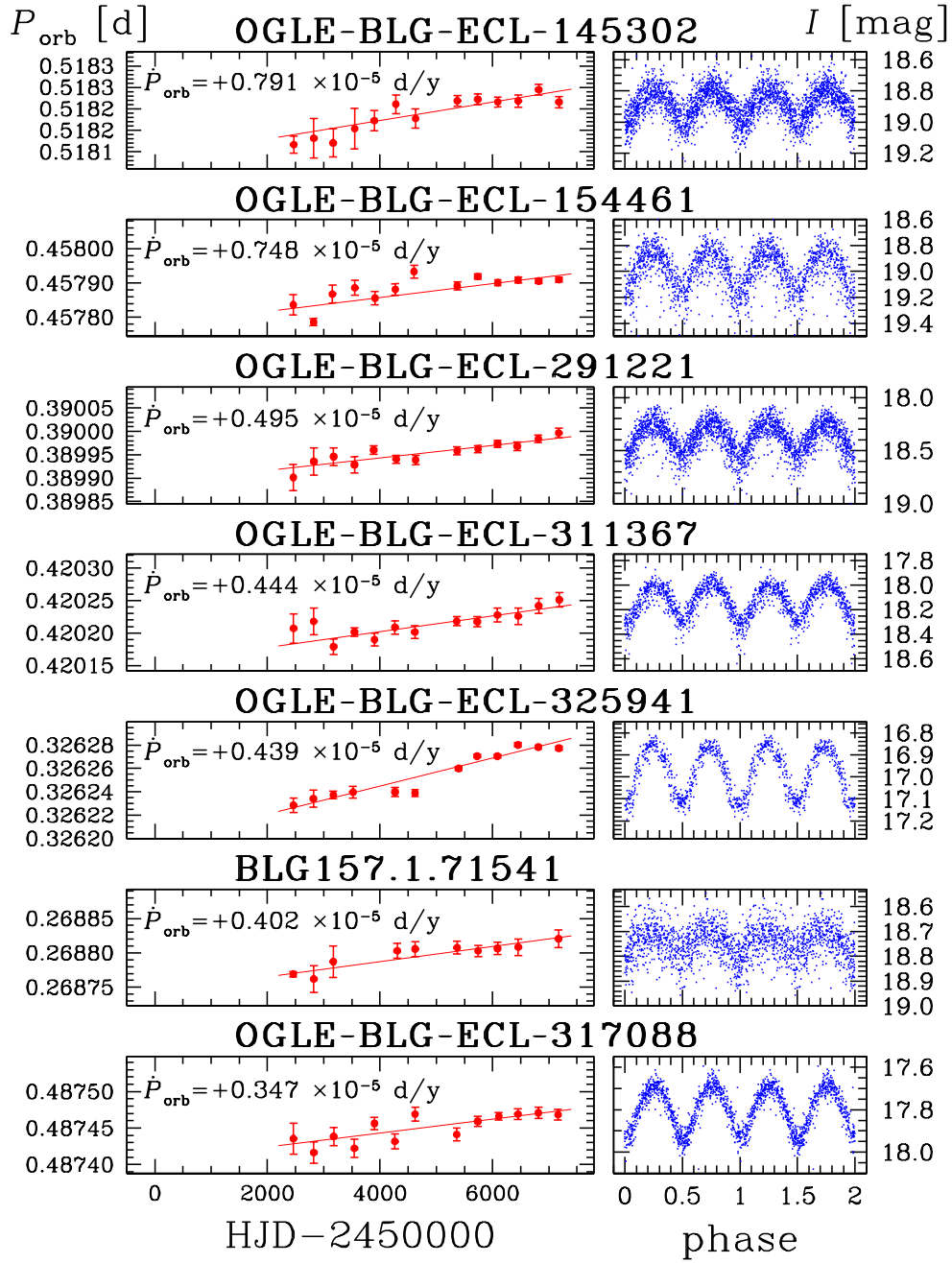


Fig. 3. Binary systems with the highest positive period change rates. OGLE-III light curves are presented.

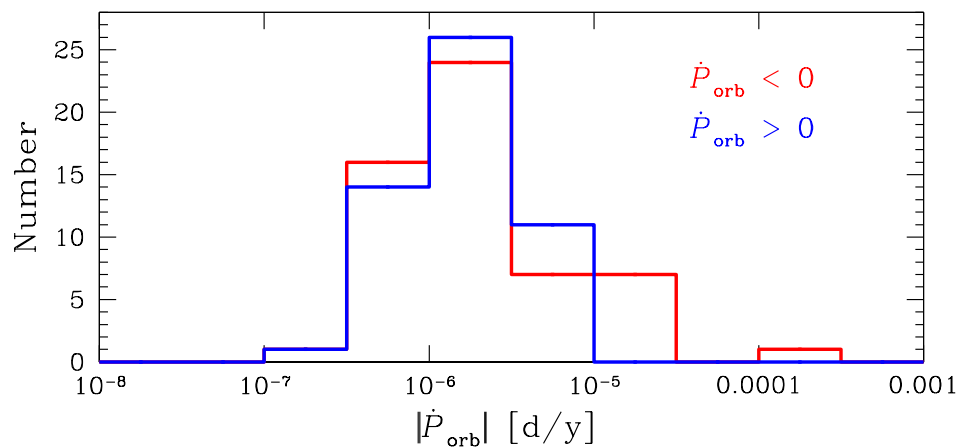


Fig. 4. Comparison of the distributions of systems with negative and positive period change rates. Note the excess of systems with high negative rate.

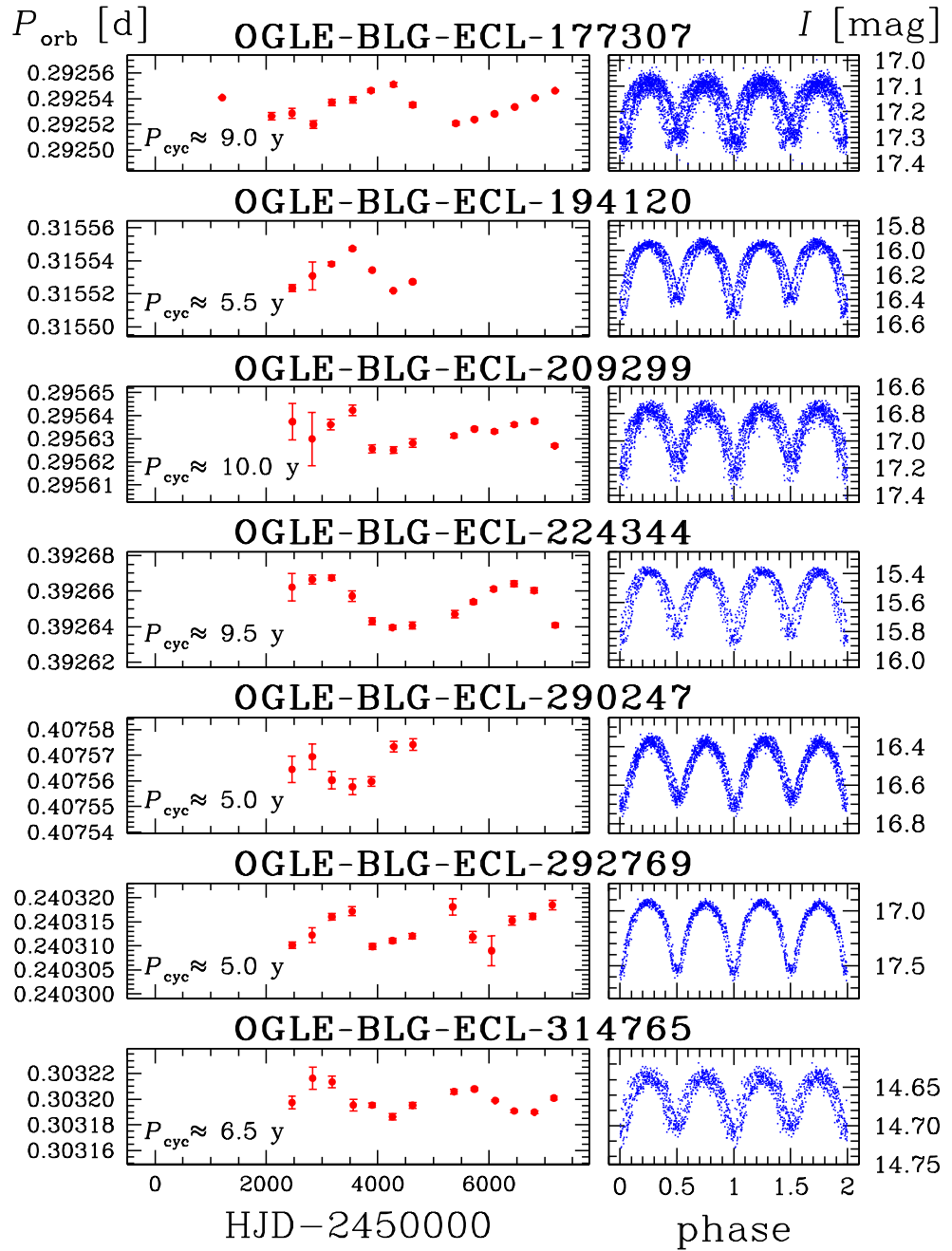


Fig. 5. Example binary systems with cyclic orbital period variations. OGLE-III light curves are phased with constant period determined for this dataset.

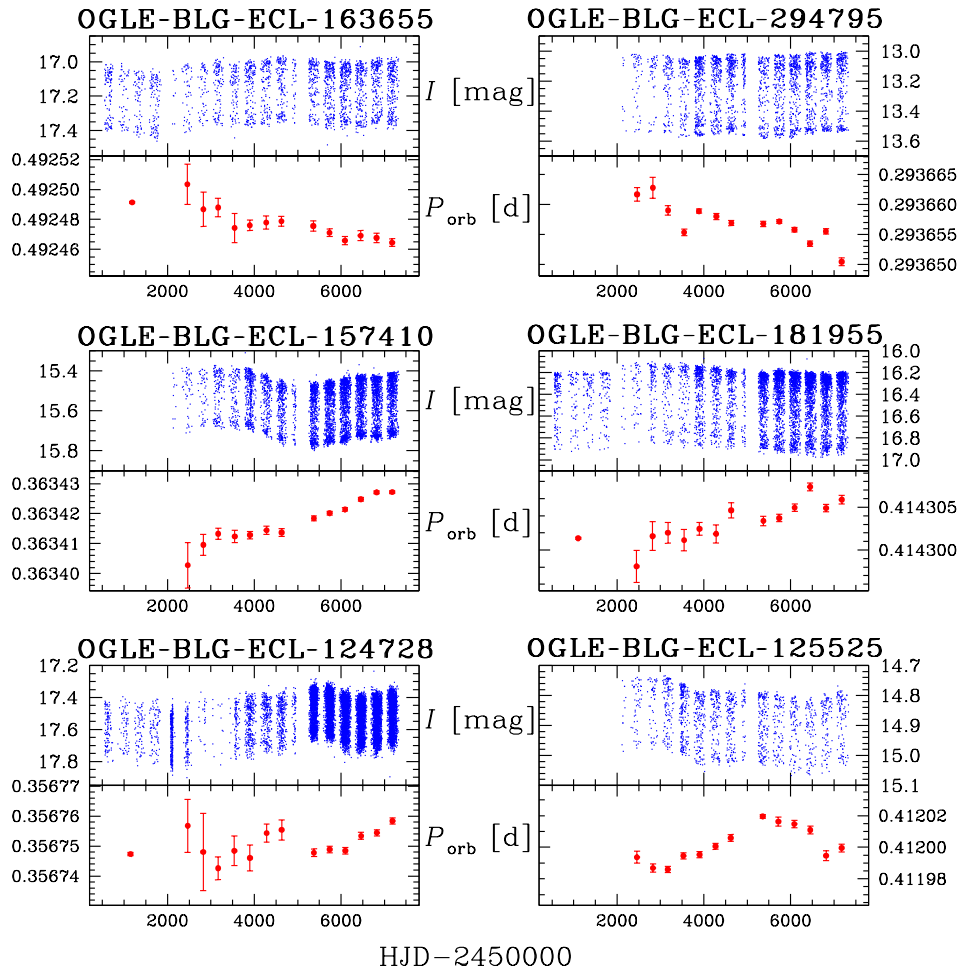


Fig. 6. Long-term brightness variations in selected binary systems with negative (upper panels), positive (middle panels), and cyclic period changes (lower panels). In some cases, the brightness variations seem to correlate with the period changes. All stars are isolated objects in the OGLE images.